Exploring commercial GNSS RO products for Planetary Boundary Layer studies in the Arctic

Manisha Ganeshan[1,2], Dong L. Wu[1], Joseph Santanello[3], Jie Gong[1], Chi Ao[4], Panagiotis Vergados[4] and Kevin Nelson[4]

[1]Climate and Radiation Laboratory, NASA Goddard Space Flight Center, Greenbelt, 20771, USA
[2]Morgan State University, Baltimore, 21251, USA
[3]Hydrological Sciences Laboratory, NASA Goddard Space Flight Center, Greenbelt, 20771, USA
[4]NASA Jet Propulsion Laboratory, California Institute of Technology, Pasadena, 91109, USA

Correspondence to: Manisha Ganeshan (manisha.ganeshan@nasa.gov)

Abstract.

Commercial Radio Occultation (RO) satellites that track radio signals from the Global Navigation Satellite System (GNSS) are being touted for their observations in polar regions where RO missions such as COSMIC-2 lack orbital coverage. This study seeks to explore the value of commercial RO satellites, viz. Spire and GeoOptics, for planetary boundary layer (PBL) investigations in the Arctic, a region where favourable lower atmospheric penetration of GNSS RO is vital for representing the persistently shallow PBL. The lower tropospheric penetration capability of both Spire and GeoOptics over the Arctic Ocean is comparable to other RO missions such as MetOp and COSMIC-1, with nearly 80% observations reaching an altitude of 500 meters above mean sea level. A seasonal cycle in RO penetration probability, with minima occurring during the warm season, is observed in all RO datasets, except the NASA-purchased Spire data. The RO-derived monthly mean Arctic PBL height (PBLH) from Spire and GeoOptics is comparable to that retrieved from MetOp and the PBLH in Modern-Era Retrospective analysis for Research and Applications version 2 (MERRA-2). A cut-off altitude threshold of 500 meters for minimum RO penetration height is generally sufficient for representing the Arctic PBLH, however, NASA Spire data perform slightly better when 300 meters threshold is used. Arctic PBLH representation, however, is not strongly affected by the total number of available observations, minimum RO penetration altitude, or instrument type, but instead appears to be sensitive to the choice of processing algorithm used for retrieving bending angle and refractivity profiles. This is the key factor which also influences the rate of penetration loss in the lower troposphere.

1 Introduction

The planetary boundary layer (PBL) is a target observable of broad importance to the Earth Science community. The Global Navigation Satellite System (GNSS) Radio Occultation (RO) has been shown to be a good candidate for observing the PBL height (PBLH) across various spatiotemporal scales (Ao et al., 2012; Basha and Ratnam, 2009; Ding et al., 2021; Kalmus et al., 2022; Nelson et al., 2021; Winning et al., 2017) as recommended by the National Academies of Science Decadal Survey

Deleted: Region
Deleted: Both Spire and GeoOptics have seemingly improved
Deleted: ed
Deleted: Spire having nearly one order (two orders) of magnitude greater volume of
Deleted: at
Deleted: compared to MetOp (GeoOptics)
Deleted:
Deleted: as well as
Deleted: the
Deleted: The PBLH retrieved from NASA-purchased Spire data has relatively less spatial and seasonal variability compared to other datasets.
Deleted: work
Deleted: ly well
Deleted: in all datasets except for
Deleted: -purchased
Deleted: which
Deleted: s
Deleted: the
Deleted: as well as the PBLH representation

for Earth Science and Applications from Space report (NASEM, 2018; Teixeira et al., 2021). Today, advancing PBL science is inherently reliant on high resolution observations with high-frequency sampling that can chiefly be afforded by a single remote sensing instrument/combination of instruments from space. In this regard, GNSS RO is a vital measurement technique, due to its superior vertical resolution (< 100 m) and viewing geometry compared to most other nadir-viewing space-based instrument technologies, allowing penetration down to 100 meters above surface. High vertical resolution measurements and deep penetration of observations into the lower atmosphere are deemed vital for polar regions, where it is particularly difficult to observe and characterize the persistent surface-based PBL temperature inversions.

1.1 Importance of GNSS RO for Arctic PBL studies: Why commercial data?

The study of the Arctic Ocean PBL can greatly benefit from GNSS RO observations, which offer: (a) continuous sampling under all weather conditions, (b) the ability to observe beneath the persistent stratus cloud cover, (c) improved performance over flat surfaces (sea ice, open ocean) compared to sharp varying slopes (land mass), and (d) a long-term data record spanning more than two decades with added coverage from recently launched commercial satellites. Commercial satellites are particularly advantageous for high-latitude polar studies where there is a notable lapse in coverage following the decommissioning of the Constellation Observing System for Meteorology Ionosphere and Climate (COSMIC-1) in 2019. The follow-on mission to COSMIC-1, COSMIC-2, only covers 45°N to 45°S. It is expected that coverage from private sector GNSS RO satellites fills the gaps in the climate data record. First, however, it is necessary to explore the lower atmospheric sounding capability of these commercial missions in comparison to past and current existing operational GNSS RO products in the Arctic, where the gradient method used for determining the PBL height (Ao et al., 2012; Nelson et al., 2021; Qiu et al., 2023; Seidel et al., 2010, 2012) is found to be sensitive to the penetration capability of RO profiles (Ganeshan and Wu, 2015). From the analysis of 8 years of COSMIC-1 data, it was found that availability of RO profiles over the Arctic Ocean reduced significantly at tangent heights below 1km, which introduces a sensitivity of the retrieved PBL height to the choice of the cut-off altitude, or minimum RO penetration depth, used for profile selection. However, it was noted that only the absolute PBLH values were sensitive to the choice of cut-off altitude, whereas the spatial and seasonal variability remained largely unaffected (Ganeshan and Wu, 2015). Thus, it is worthwhile to exploring the lower atmospheric penetration capability of commercial RO products and their representation of the Arctic PBLH compared to other established climate datasets.

Deleted: Regardless

Deleted: compare

Deleted: among various GNSS RO products

Deleted: and to explore factors that can influence this capability, and in turn, influence the

Deleted: observat

Deleted: ion of

1.2 A background of GNSS RO neutral atmosphere technique

In the GNSS RO technique, the neutral atmosphere is considered as the atmospheric path consisting of the troposphere and stratosphere (up to 60 km) which is refractive and electrically neutral, unlike the mesosphere and ionosphere-thermosphere regions. The neutral atmosphere has both dry and wet components that contribute to the refraction, with the wet component becoming more important closer to the surface due to increased concentrations of water vapor. Not all RO profiles reach the surface, and in fact, there can be an exponential drop in the fraction of available RO observations (penetration probability) as we go towards the surface (Ganeshan and Wu, 2015) which is primarily due to the decrease in the signal-to-noise ratio (SNR) caused by atmospheric defocusing (Wu et al., 2022). However, factors such as instrument design, neutral atmosphere excess phase computation method, and choice of bending angle retrieval algorithm can also affect the penetration probability profile for a given atmospheric path.

A thorough understanding of factors affecting RO penetration is desirable to help minimize sampling bias as well as to ensure data continuity and consistency in climate records. However, this is difficult to achieve, given the existence of a large number of GNSS RO missions and different versions of products from a single mission that are periodically reprocessed to remain up to date with advances in software and processing algorithms. This study aims to provide a comparison of the penetration capability of new commercial GNSS RO data products against other existing products in the Arctic as the first step towards establishing a climate ready, long-term continuous, dataset that can be used for Arctic PBL investigations.

2 Data and Methodology

2.1 GNSS RO

2.1.1. Commercial RO Datasets

The goal of this study is to explore the value of commercial GNSS RO products for PBL studies in the Arctic Ocean (north of 60°N excluding land areas) by comparing with other GNSS RO mission products such as, COSMIC-1 and the Meteorological Operational satellite programme (MetOp). The commercial GNSS RO data evaluated in this study are purchased by NASA through the Commercial SmallSat Data Acquisition (CSDA) program. In addition, this study also compares freely available commercial data purchased for near-real time operations by NOAA, for available periods of overlap with the NASA- purchased commercial data.

NASA-purchased Spire data are available from November 2019 through June 2024, and NASA-purchased GeoOptics data are available from January 2020 to April 2021. Spire data are provided at a similar vertical grid and resolution as other GNSS RO missions (such as COSMIC, COSMIC-2, and MetOp) where the lowest level of valid observations differs from profile to profile, because the penetration depth achieved by each RO is unique, depending primarily on the SNR. GeoOptics data, on the other hand, are provided on a uniform 100 m vertical grid, along with a quality flag that is used to determine the lowest penetration level. GeoOptics uses the phase matching methodology in RO processing (Jensen et al., 2004), a wave optics technique designed to extract the full information from the received wave field. The quality flag is applied in two ways: (i) blanket criteria that checks the range of the amplitude of computed phase matching integral and cumulative number of phase jumps within the upper neutral atmosphere (between 8 to 40 km), cutting off the profile at lower levels if the above checks are failed, and (ii) individual criteria that flag each level as "good" or "bad" based on the presence or absence of sharp features (moisture and temperature gradients) that can cause significant deviation of the bending angle relative to a smoothed background bending angle profile. In this study, only profiles satisfying the blanket criteria are considered as the focus is on

Deleted: a

Deleted: uary

Deleted: 2

the lower troposphere (surface to 5 km). Moreover, each of these profiles are evaluated individually to determine the minimum penetration depth ascertained by the lowest above-surface level with a “good” quality flag. It is important to note that if a “sharp” PBL inversion layer with poor quality control (QC) flag exists above the minimum penetration depth, that profile is not discarded.

The NOAA Spire and GeoOptics data purchased for near-real time operations are downloaded from the University Corporation for Atmospheric Research (UCAR; http://www.cosmic.ucar.edu/) website. NOAA purchases Level 1b (L1B) data from both vendors and the Level 2 (L2) neutral atmosphere products are retrieved from in-house excess phase computations carried out by UCAR in near-real time. In the case of GeoOptics, the overlap between NOAA and NASA data is during the month of April 2021, and for Spire, the month of October 2021 is chosen to compare overlapping data. All references to “Spire” and “GeoOptics” in this paper imply NASA purchased commercial RO data unless explicitly specified to be NOAA-purchased datasets.

2.1.2. Other datasets

A major focus of this study will be the comparisons between three datasets, viz. NASA Spire, NASA GeoOptics, and the re-processed EUMETSAT MetOp data from the Radio Occultation Meteorology Satellite Applications Facility (ROM SAF). The MetOp data are part of the Interim Climate Data Record (ICDR) ROM SAF product which was developed in 2017. Although MetOP near-realtime (NRT) product from ROM SAF has more advanced processing setup with improved lower tropospheric penetration, the goal is to compare with a consistent climate record to avoid ambiguities resulting from frequent software updates. Therefore, the ICDR data are used in this study. Some differences are observed between the rising and setting occultations of MetOp data owing to the use of raw sampling tracking which is not considered full “open loop” tracking. In this study, we only consider setting occultations from MetOp which are known to have slightly better SNR and an overall deeper penetration (Innerkofler et al. 2023). Additionally, re-processed data from COSMIC-1 available from the University Corporation for Atmospheric Research (UCAR) are used to compare RO penetration statistics over the Arctic. COSMIC-1 data ceased to be produced beyond 2019, thereby limiting their use for this comparative analysis which is mainly focused on the year 2020. For this study, they serve to provide a stable climatological record of RO penetration statistics over the Arctic Ocean against which characteristics of newer datasets can be compared. Two versions of UCAR reprocessed COSMIC-1 data (from the year 2013 and the year 2021) are obtained for the period ranging from 2007 to 2013 and from 2007 to 2017, respectively. Table 1 lists and describes all RO datasets used in this study, including the center where the L2 data are processed.

Deleted: contemporaneous

Deleted: In addition

Deleted: and COSMIC-2 data

Deleted: from

Deleted: will be

Deleted: 2013.3520

Deleted: .0390

Deleted: COSMIC-1 data ceased to be produced beyond 2019, thereby limiting their use for this comparative analysis which is focused on the year 2020. For this study, they serve as a climatological record of RO penetration statistics over the Arctic Ocean against which characteristics of newer datasets can be compared. To remove ambiguity resulting from software updates - and to ensure consistency - only those RO mission products that have been re-processed with the same software version are compared against Spire and GeoOptics.

Satellite Product	**Processing center**	**Data period**	**Monthly avg. #RO profiles over Arctic Ocean**	**Data Version**	**Processing mode**
MetOp ICDR	ROM SAF	2020, Apr 2021, Oct 2021	1974	ICDR	Reprocessed
COSMIC 2013	UCAR	2007-2013 (only Apr and Oct)	3503	2013.3520	Reprocessed
COSMIC 2021	UCAR	2007-2017 (only Apr and Oct)	2904	2021.0390	Reprocessed
NASA Spire	Spire	2020, Oct 2021, Feb 2024	17207	Version 06	Vendor provided
NOAA Spire	UCAR	Oct 2021, Feb 2024	6223	-	Near Real-Time
NASA GeoOptics	GeoOptics	2020, Apr 2021	754	Version 01	Vendor provided
NOAA GeoOptics	UCAR	Apr 2021	3250	-	Near Real-Time

Table 1. List of all RO satellite products used in this study, along with the chosen study period and the average monthly RO profile count over the Arctic Ocean during the study period.

2.1.3. Deriving PBLH from GNSS RO

The PBLH is derived from the GNSS RO refractivity profile using the bottom-up search approach described in Ganeshan and Wu (2015), identifying the first minima of the refractivity gradient to exceed -40 N-unit km^{-1} and assigning the corresponding altitude as the PBLH. This approach is specifically useful for deriving the height of the PBL inversion over the Arctic during winter months. A cut-off altitude threshold (which is a required minimum penetration threshold), typically set to 500 m (Ao et al., 2012, Guo et al., 2011, Ganeshan and Wu, 2015), is applied to only include RO profiles that reach this altitude or lower. Ganeshan and Wu (2015) showed that even though the magnitude of the retrieved PBLH over Arctic is sensitive to the cut-off altitude, its spatiotemporal variability remained unaffected by the choice of this threshold. In this study, sensitivity of commercial RO products to the choice of cut-off altitude threshold will be additionally explored. All GNSS RO derived monthly mean penetration probability and monthly PBL height characteristics are interpolated onto a 2° latitude x 10° longitude grid, as in Ganeshan and Wu (2015). A distance-weighted averaging method is used for interpolation by considering observations falling within a circle of 5° around each grid point.

Deleted: ,

Deleted: This is the typical cut-off altitude used for GNSS RO based PBL studies (Ao et al., 2012, Guo et al., 2011) that has also proven useful for Arctic PBLH retrieval (Ganeshan and Wu, 2015).

Deleted: A nine-point local smoothing is further performed on PBLH values derived from GeoOptics and MetOp observations to help minimize random variations due to smaller sample size.

2.2 Reanalysis Data

The MERRA-2 reanalysis product (Gelaro et al., 2017) is used to obtain the monthly mean PBL height and the monthly mean sea ice fraction over the Arctic Ocean. In MERRA-2, the PBL depth is defined as the model level where the eddy heat diffusivity coefficient (K_H) value falls below 2 $m^2\ s^{-1}$ threshold (McGrath-Spangler et al., 2015). The GEOS atmospheric model used in MERRA-2 includes separate parameterizations for stable and unstable PBLs. The non-local Lock et al. (2000) scheme is used to parameterize turbulence in unstable boundary layers, whereas, the model employs a first-order local turbulence closure scheme, Louis et al. (1982), for stable boundary layers. The Louis scheme is expected to be more active in regions such as the Arctic Ocean which are typically characterized by stable conditions. The scheme estimates heat and momentum diffusivity coefficients based on the turbulent length scale and bulk Richardson number at each time step wherein the former is determined by the PBL depth from the previous time step (Ganeshan and Yang, 2019). In case of persistent stable conditions, such as over the frozen Arctic Ocean, the turbulent length scales are expectedly small, implying that the model diffusivity coefficients are largely based on the bulk Richardson number. Thus, MERRA-2 PBLH over Arctic is inherently sensitive to wind and temperature gradients (used for computing the bulk Richardson number), making it comparable to the PBL temperature inversion which is detected by GNSS RO.

In general, the first model level over the Arctic Ocean is around 50 meters above surface and the vertical grid spacing is approximately 100 meters within the lowest five model levels. The horizontal resolution of MERRA-2 products is approximately ~0.5 degrees. The MERRA-2 variables are similarly interpolated onto the 2°x10° horizontal grid (described in section 2.1.3), for ease of comparison. The MERRA-2 vertical grid is based on a terrain-following sigma coordinate system.

3 Results and Discussion

3.1 Sensitivity of RO penetration loss to bending angle retrieval method

GNSS RO bending angle and refractivity profile observations are characterized by a loss of signal (decrease in SNR) as they approach the surface due to atmospheric defocusing (Wu et al., 2022). However, the rate of penetration loss is expectedly different for various RO missions, due to diversity in the design of GNSS receivers and SNR capabilities. Penetration loss can also be different for measurements from the same instrument, due to inherent disparity in excess phase computations and bending angle retrieval algorithms. For example, older versions of the same product, such as the UCAR COSMIC 2013 version, can differ significantly from newer reprocessed versions (e.g., COSMIC 2021 version), due to advances in excess phase computations, retrieval software, GNSS orbits, clock, and earth orientation products (UCAR Data Release, 2022).

Figure 1 compares the rate of RO penetration loss over the Arctic Ocean for different GNSS RO missions (COSMIC, MetOp, Spire) as well as for different products from the same mission (e.g., COSMIC 2013 vs. COSMIC 2021; Spire NASA vs. Spire NOAA). Clearly, the penetration loss is much less significant for the newer version of COSMIC-1 data compared to the older version, due to major advances in computations and retrieval software. The penetration probability is more or less

Deleted: -1
Deleted: .3520
Deleted: -1
Deleted: .0390
Deleted: , GeoOptics
Deleted: -1
Deleted: .3520
Deleted: -1
Deleted: .0390
Deleted: ; GeoOptics NASA vs. GeoOptics NOAA

similar for both the Spire, MetOp, and COSMIC 2021 products, with differences generally being confined to the lowest 1 km. Spire NASA and MetOp penetration probabilities behave similarly. On the other hand, Spire NOAA data are similar to the reprocessed COSMIC 2021 product despite differences in SNR between the two, with more than 50% of the profiles penetrating down to 100 m above the surface, as opposed to less than 5% for MetOp and Spire NASA data. The average number of monthly observations for each data product is shown in Table 1.

It is conceivable that differences between Spire NASA and Spire NOAA products in Fig. 1 (left panel) could be attributable to the differences in the volume and sample size of available data (for example, Table 1), however, this is not found to be the case. Figure 1 (right panel) shows the RO penetration probability for a common subset consisting of the exact sub-sample of Spire RO profiles but processed by different sources. The former is processed by the vendor and purchased by NASA as L2 product, while the latter is processed by UCAR from the vendor provided L1b data. Even though the same physical ROs are compared, the two products show distinctive penetration patterns below 500 meters. The penetration probabilities differ solely due to the choice of processing algorithm used for retrieving the bending angle and refractivity profiles. On the contrary, when comparing NOAA Spire profiles with COSMIC 2021 profiles, both processed by UCAR, there is little to no difference in the penetration probabilities (Fig. 1(a)). Thus, processing software appears to have a greater bearing on RO penetration loss compared to instrument hardware.

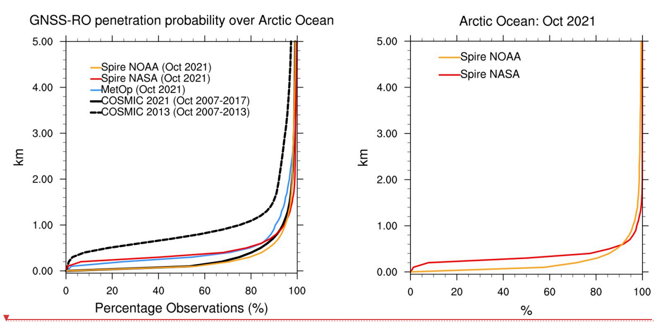

Fig. 1 RO penetration loss as a function of altitude over the Arctic Ocean (north of 60°N) for the month of October 2021 comparing **(left)** different product versions from three major missions viz., COSMIC-1, MetOp, and Spire and **(right)** a common sub-sample from Spire NASA and Spire NOAA over the Arctic Ocean.

Similarly, Figure 2 compares the RO penetration profiles for GeoOptics, MetOp and COSMIC-1 missions. Once again, the most significant differences in RO penetration probabilities are between the old and new reprocessed versions of COSMIC-1 data. Relatively, a fewer percentage of GeoOptics profiles reach 5 km altitude, likely due to the imposed quality checks

Deleted: Clearly, the penetration loss is less significant for the newer version of COSMIC-1 data compared to the older version, due to major advances in computations and retrieval software. For contemporaneously processed commercial data products, viz. Spire NASA vs Spire NOAA and/or GeoOptics NASA vs. GeoOptics NOAA, the differences in penetration probability are generally confined to the lowest 1 km.

Deleted: These

Deleted: are solely due to the choice of processing algorithm used for retrieving the bending angle and refractivity profiles. The Spire NOAA data are similar to the reprocessed COSMIC-1 2021.0390 data, despite differences in SNR between the two products, with more than 50% of the profiles penetrating down to 200 m above the surface, as opposed to less than 5% for MetOp and Spire NASA data. ¶

Deleted: 2 (a)

Deleted: NASA-purchased and NOAA-purchased Spire profiles

Deleted: purchased

Deleted: -2

Deleted: over the tropics

Deleted: 2

Deleted: b

Formatted: Indent: First line: 0"

Deleted:

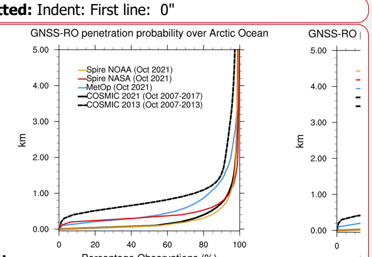

Deleted: from different products

Deleted: (left)

Deleted: for the month of October

Deleted: COSMIC-1, MetOp, and GeoOptics for the month of April…

described in section 2.1.1, however, a good percentage of observations (more than 50%) reach 100m altitude, which is comparable to the 2021 reprocessed COSMIC-1 product.

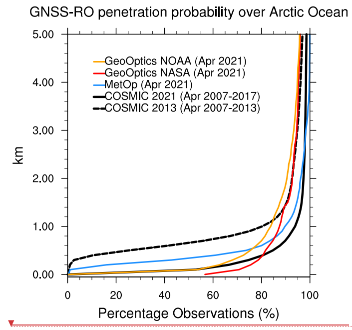

Fig. 2 RO penetration loss as a function of altitude over the Arctic Ocean (north of 60°N) for the month of April 2021 comparing different product versions from three major missions viz., COSMIC-1, MetOp, and GeoOptics.

3.2 Comparison of RO penetration over the Arctic Ocean

The top row of Figure 3 compares the minimum altitude of RO penetration over the Arctic Ocean for NASA Spire, NASA GeoOptics, and MetOp data. Spire and MetOp have similar RO penetration depth throughout the Arctic Ocean, with values dropping towards continental coastlines which is expected due to influence of topography. GeoOptics has the lowest and highest values of minimum RO penetration altitude compared to the other two datasets, with the lows occurring over the frozen ocean in the Beaufort Sea region and to the north of Greenland, and the highs occurring over the Atlantic storm track region. A similar pattern of enhanced RO penetration loss in the storm track region was also observed in COSMIC-1 (2013 version product; Ganeshan and Wu, 2015). It has been previously speculated (Ao et al., 2012; Ganeshan and Wu, 2015; Chang et al., 2022) that there is an inverse relationship between water vapor amount and RO penetration depth, with increased lower atmospheric penetration typically observed in regions away from the tropics, specifically over the dry north pole.

Deleted:

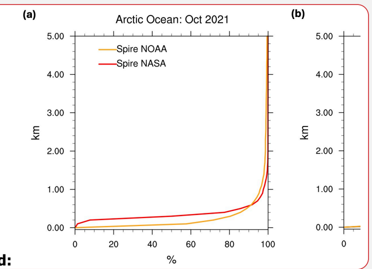

Deleted: RO penetration loss as a function of altitude for October 2021 showing **(a)** differences in penetration probabilities for a common subset of monthly ROs over the Arctic Ocean obtained from a single mission/instrument (Spire) processed by different centers and **(b)** similarities in penetration probabilities for different sources of monthly ROs over the Tropics (30°S to 30°N) obtained from two separate missions but processed by the same center (UCAR)….

Deleted: s

Deleted: deeper

Deleted: compared to MetOp

Deleted: which is expected, due to the less pronounced rate of loss of penetration below 3 km

Deleted:

Deleted: (as seen in Fig. 1)

Deleted: data

Deleted: (

Deleted: The minimum penetration capability of MetOp is higher over the frozen Arctic Ocean compared to the open ice-free ocean, a pattern that was similarly observed for COSMIC-1 data (Ganeshan and Wu, 2015).

Deleted: The minimum penetration depth from Spire is more spatially homogeneous compared to the other two data sets, showing less sensitivity to surface properties and meteorology.

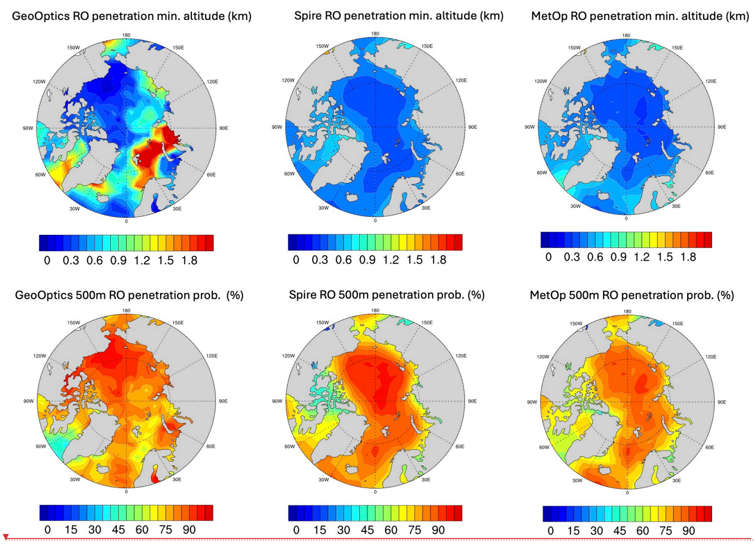

Fig. 3 RO penetration statistics over the Arctic Ocean for December 2020 comparing GeoOptics, Spire and MetOp datasets showing **(top)** the minimum altitude of RO penetration and **(bottom)** the RO penetration probability at 500 m altitude.

Previous studies (Ao et al. 2012; Ganeshan and Wu, 2015), have typically chosen a 500 m cut-off altitude to select RO profiles for retrieving the PBLH. Figure 3 (bottom row) compares the RO penetration probability at 500 m altitude between the three datasets. In general, all three products have a high fraction of RO observations (~80%) reaching 500 meters altitude. Figure 4 compares the time-series of total number of available RO observations at 500 m altitude over the Arctic Ocean. We note a reduction of MetOp and GeoOptics RO profiles during summer months which are, once again, indicative of sensitivity to atmospheric moisture (Ao et al., 2012; Ganeshan and Wu, 2015; Chang et al., 2022). NASA Spire profiles, however, do not show a similar response to moisture, albeit NOAA Spire profiles have the same seasonality in RO penetration probability (not shown). Nevertheless, the focus of this study is winter season (November-April) during which all three datasets have similar penetration characteristics.

Deleted: 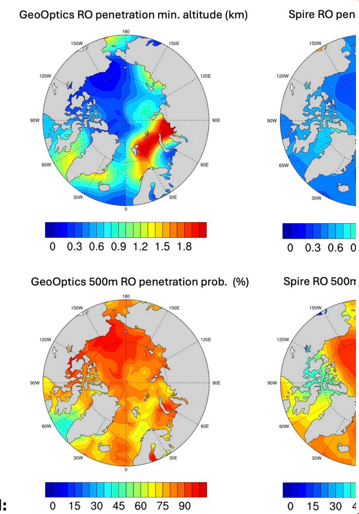

Deleted: Based on

Deleted: p

Deleted:

Deleted: involving RO-derived PBLH

Deleted: is chosen

Deleted: used

Deleted: both commercial

Deleted: compared to MetOp (~60%)

Deleted: ¶
¶

Deleted: Spire has the maximum number of daily observations, nearly an order (two orders) of magnitude greater than MetOp (GeoOptics). ...

Deleted: in

Deleted: more stringent quality control criteria

Deleted: ,

Deleted: and a similar drop in GeoOptics RO profiles in February, June, and October

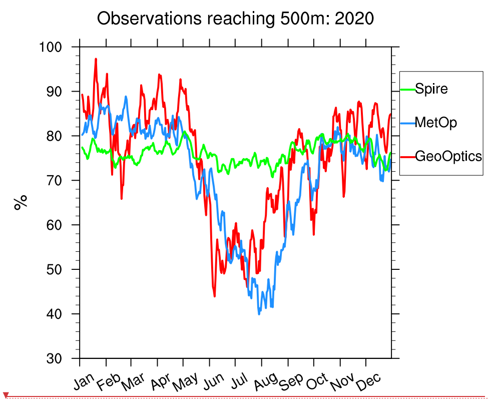

Fig. 4 Annual time-series of percentage of RO observations reaching 500 m altitude or lower over the Arctic Ocean for the year 2020. The daily observations are smoothed using a 5-day running average filter.

3.3 Performance of commercial GNSS RO datasets for Arctic Ocean PBLH retrieval

This section will focus on exploring the potential for using commercial RO data for Arctic winter PBL studies. As a first step, the cut-off altitude threshold of 500 m is chosen to select RO profiles, which has been used in previous studies (see section 2.1.3 and section 3.1). Ganeshan and Wu (2015) showed that the minimum refractivity gradient method works well to detect the height of PBL temperature inversions over the Arctic Ocean during winter months (November – April). Due to the lack of moisture in the atmosphere, the refractivity gradient minimum is found to be sensitive to the positive temperature gradient maxima (i.e. temperature inversions).

Figures 5-7 compare the monthly RO-derived PBLH characteristics for each product during the cold season months of the year 2020 (January – April, and November – December). The adopted methodology (Ganeshan and Wu, 2015) described in section 2.1.3, appears to work well for all three RO products, which clearly show the expected distribution of shallow PBLH over sea ice versus deeper PBLH over the Atlantic sector (monthly sea ice distributions shown in Figure 8). The extreme high values of PBLH estimates in the Atlantic Sector, especially seen in GeoOptics and MetOp data, seem to be related to expected storm activity in this region. A seasonal evolution in the retrieved PBLH is evident in both GeoOptics and MetOp datasets with the lowest values generally observed during January, February and March, and highest values in November, which is in agreement with MERRA-2 derived PBLH (Figure 9). On the other hand, NASA Spire derived mean PBLH appears to have lesser spatial and seasonal variation compared to the other two datasets and compared to MERRA-2, which could be because of the increased

Deleted: 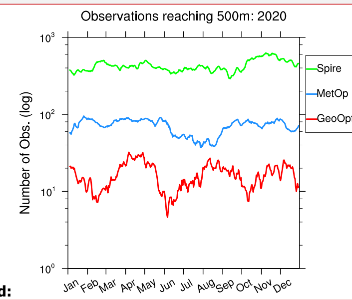

Deleted: number

Deleted: refractivity-based PBLH over

Deleted: using

Deleted: described previously

Deleted: GeoOptics and MetOp

Deleted: based on

Deleted: , with GeoOptics showing a stronger contrast between the two regions

Deleted: GeoOptics

Deleted: s

Deleted: the

Deleted: high minimum penetration altitude

Deleted: in this region

Deleted: (seen in top row of Fig. 3)

Deleted: good

vertical smoothing applied to their bending angle product (Bowler, 2020) that may limit the effective vertical resolution of refractivity and the range of refractivity-derived PBLH values.

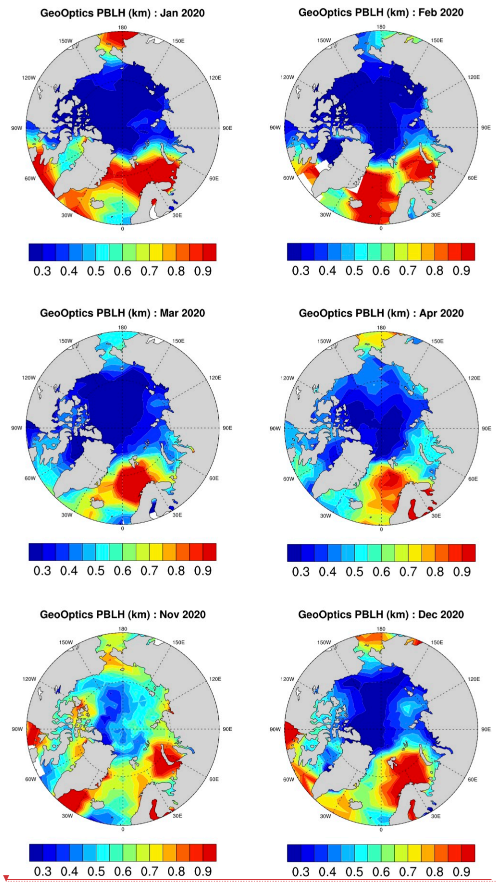

Fig. 5 NASA GeoOptics monthly Arctic PBLH for cold season months of the year 2020.

Deleted:

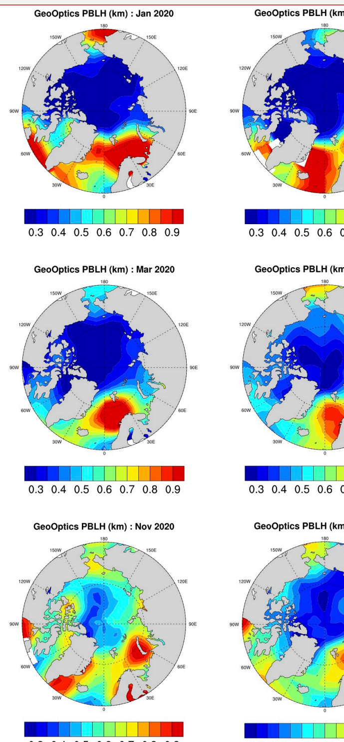

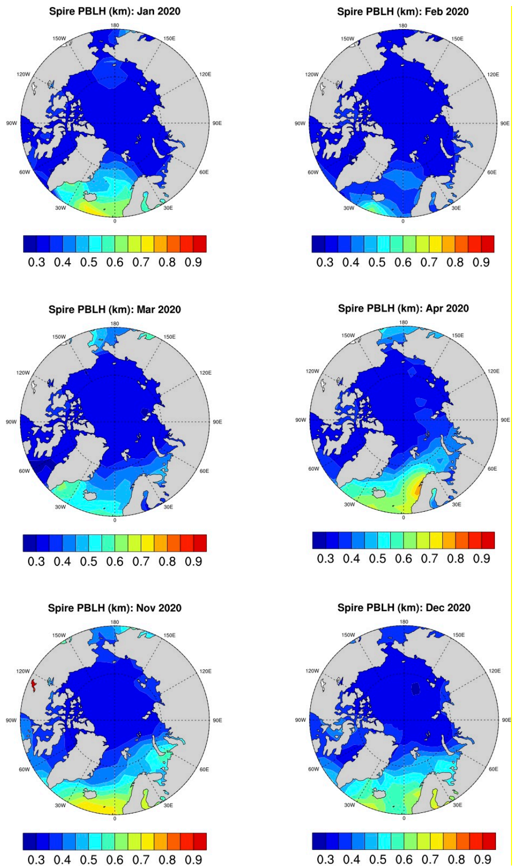

Fig. 6 NASA Spire monthly Arctic PBLH for cold season months of the year 2020.

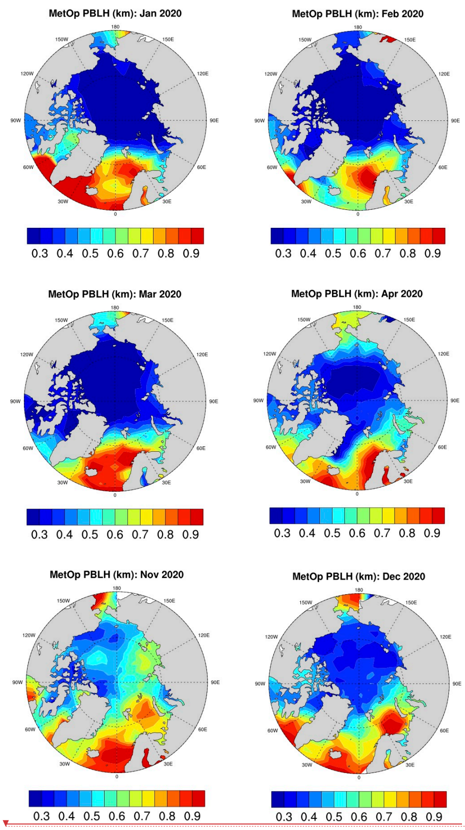

Fig. 7 MetOP monthly Arctic PBLH for cold season months of the year 2020.

Deleted:

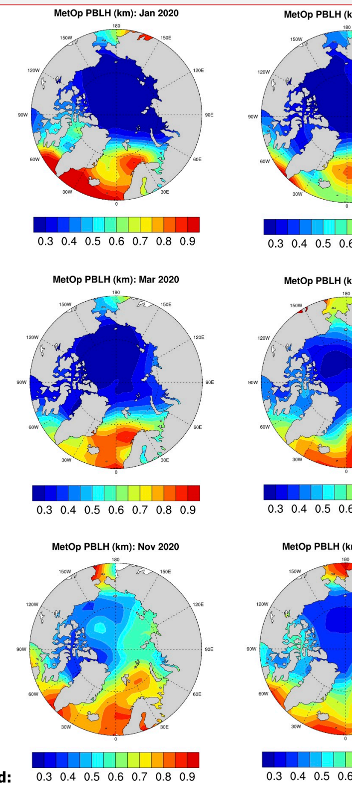

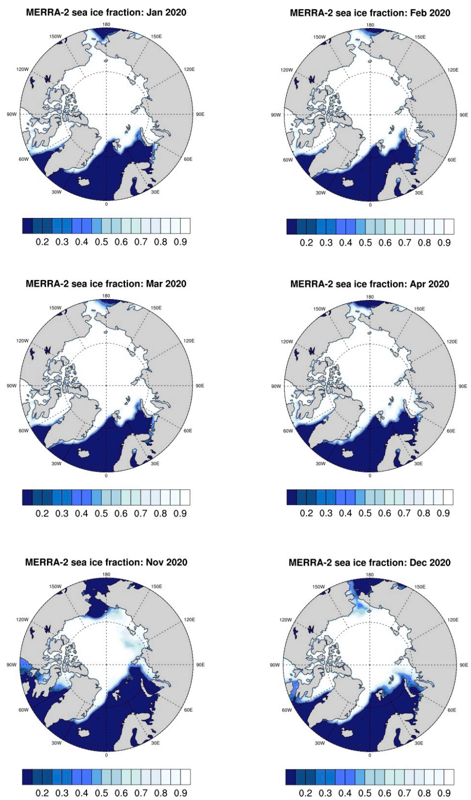

Fig. 8 MERRA-2 monthly Arctic sea-ice fraction for cold season months of the year 2020.

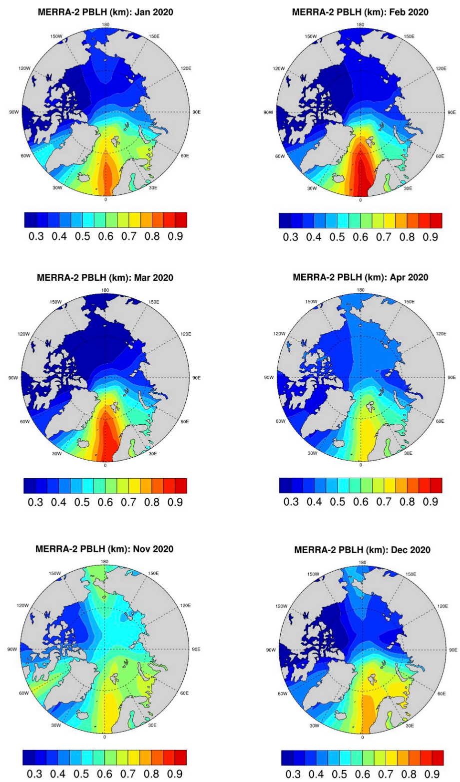

Fig. 9 MERRA-2 monthly PBLH showing the seasonal evolution and spatial variability of Arctic PBLH for cold season months of the year 2020.

3.4 Sensitivity to cut-off altitude threshold

As discussed in Ganeshan and Wu (2015), a sampling bias may occur in the retrieved PBLH due to a sharp drop in available RO profiles (as seen for COSMIC-1 2013 version in Fig. 1), thereby necessitating the selection of an optimal cut-off altitude threshold for minimum required RO penetration height. Although the penetration probability is much improved for commercial RO observations compared to COSMIC-1 2013 product, with more than three factor increase in the percentage of observations reaching 500 m altitude, it is still possible that some shallow PBLs are missed. Particularly, in the case of NASA-purchased

Deleted: explained in section 1.2,

Deleted: ny

Formatted: Justified

Deleted: the standard cut-off altitude

Deleted: of 500 m

Deleted: has been regarded as sufficient for deriving refractivity-based PBLH from COSMIC RO observations in the Arctic, it has been noted to be less than ideal for inferring PBL depth in the case of shallow PBLs (Ao et al., 2012) and may even contribute to a positive bias in regions such as the central Arctic Ocean (Ganeshan and Wu, 2015). It appears, however, that the 500 m cut-off altitude when applied to NASA-purchased GeoOptics and MetOp data is adequate to obtain a realistic representation of the shallow Arctic PBLH. I

Spire data, the derived PBLH values are slightly higher compared to the other two RO datasets and MERRA-2 reanalyses (Fig. 6). It is worth investigating whether the standard 500 m cut-off altitude is suboptimal for NASA-purchased Spire data. Additionally, it is also possible that NOAA Spire refractivity profiles, which are processed using UCAR software on vendor provided L1b data, data have better performance in capturing the shallow Arctic PBLH.

Figure 10 shows the PBLH retrievals from NASA Spire computed using the standard cut-off altitude threshold of 500 m (left panel) and a lower cut-off altitude threshold of 300 m (middle panel), and the resulting PBLH is indeed found to be shallower when using a lower cut-off altitude threshold. Despite an improvement in the PBLH magnitude, the coarse spatial gradients and lacking seasonal variability (seen in Fig. 6) continue to persist even after using a lower cut-off altitude threshold (not shown). On the other hand, the Arctic PBLH derived using the NOAA-purchased Spire data using the standard cut-off altitude threshold of 500 m (right panel of Fig. 10), is able to better capture the shallower PBLs and spatial contrast between the frozen Arctic Ocean and open seas region (for example, Chukchi sea) which is missed by NASA Spire observations. Thus, an optimal cut-off altitude threshold for representing Arctic PBLH values in NASA Spire data appears to be 300 m, however, the spatiotemporal variability in the derived PBLH is not highly impacted by cut-off altitude choice. It appears that qualitative differences in Arctic PBLH representation are mostly decided by the processing set up. In summary, both commercial RO datasets viz. Spire and GeoOptics, can satisfactorily represent the Arctic PBLH.

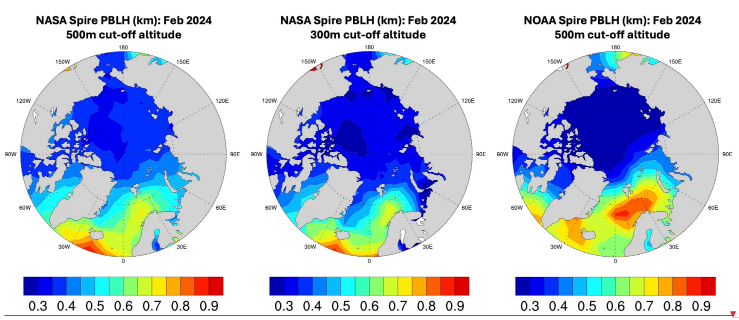

Fig. 10 RO-derived PBLH over the Arctic Ocean for February 2024 retrieved from (a) NASA Spire data using 500 m cut-of altitude threshold and (b) NASA Spire data using 300 m cut-off altitude threshold and (c) NOAA Spire data using 500 m cut-off altitude threshold for minimum RO penetration depth.

4 Summary and Conclusions

This study explores the use of commercial GNSS RO neutral atmosphere products from Spire and GeoOptics to advance Arctic PBL studies. The launch of commercial GNSS RO CubeSat receivers, such as Spire and GeoOptics, presents an unparalleled

Deleted: ¶ ¶ ... [1]
Deleted: **Fig. 10** Annual time-series of penetration probabil ... [2]
Deleted: the annual time-series of the fraction of available ... [3]
Deleted: are re
Formatted: Indent: First line: 0"
Deleted: a
Deleted: of
Deleted: values are
Deleted: significantly
Deleted: the poor granularity in its
Deleted: features
Deleted: the lack of
Deleted: as
Deleted: Figure 11
Deleted: shows
Deleted: for February 2020 comparing two sets of retrievals from
Deleted: AS
Deleted: both
Deleted: s
Deleted: (i.e.
Deleted: and 300 m)
Deleted: Even though the 300 m cut-off altitude better capt ... [4]
Deleted: In summary
Deleted: representation of
Deleted: remains unsatisfactory
Deleted: while RO penetration capability can affect the cho ... [5]
Deleted: due to different
Deleted: software versions
Deleted: Note that, unlike other datasets that show a drop i ... [6]
Deleted: ¶ ... [7]
Deleted: **1**
Deleted: PBLH
Deleted: (a)

opportunity for high-latitude PBL studies that are impacted by the loss of COSMIC-1 and the limited coverage by its successor COSMIC-2. To continue to support PBL studies in polar regions, new GNSS RO products must have sufficient lower atmospheric penetration capability, and the ability to sample shallow PBL temperature inversions that often persist in polar regions. This study attempts to provide a comparison of the penetration capability of the new commercial and other existing GNSS RO data products in the Arctic as the first step towards establishing a climate-ready, long-term continuous, dataset that can be used for Arctic PBL investigations.

It is found that the choice of processing software for retrieving neutral atmosphere bending angle and refractivity profiles has a great bearing in determining the rate of RO penetration loss in the lower troposphere, compared to factors such as instrument hardware. Both commercial products purchased by NASA are found to have comparable lower atmospheric penetration over the Arctic Ocean to other RO climate data products such as MetOp observations from ROM SAF and COSMIC-1 from UCAR. We identified that, on average, 80% of GeoOptics RO and Spire RO measurements could probe the Arctic troposphere as low as 500 meters. All RO datasets, with the exception of NASA-purchased Spire data, show a drop in the penetration probability during summer months signifying sensitivity to atmospheric water vapor which has been speculated in the past (Ao et al., 2012; Ganeshan and Wu, 2015; Chang et al., 2022).

The PBLH derived from the commercial RO products is agreeable with other RO datasets and reanalysis data. Despite its relatively low sampling volume as compared to Spire, the spatial pattern and seasonal evolution of Arctic Ocean PBLH are better represented by GeoOptics data. The Spire PBLH representation is seemingly improved when using NOAA processed L2 data, suggesting sensitivity to the choice of software used for processing L1B radiances. While there is some sensitivity to cut-off altitude threshold, it is predominantly the methodology used to obtain neutral atmosphere products from excess phase data that is ultimately crucial for Arctic PBLH representation. With that caveat, both Spire and GeoOptics show promising results for polar PBL studies.

Acknowledgments: This research was done in collaboration with Jet Propulsion Laboratory, California Institute of Technology under a contract with the National Aeronautics and Space Administration (80NM0018D0004) in addition to support from NASA grant 80NSSC23K0385. The research described in this paper was partially carried out at the Jet Propulsion Laboratory, California Institute of Technology, under a contract with the National Aeronautics and Space Administration.

Competing Interests: The contact author has declared that none of the authors has any competing interests.

References

Ao, C. O., D. E. Waliser, S. K. Chan, J.-L. Li, B. Tian, F. Xie, and A. J. Mannucci (2012). Planetary boundary layer heights from GPS radio occultationrefractivity and humidity profiles,J. Geophys. Res.,117, D16117, doi:10.1029/2012JD017598

Deleted: presently

Deleted: →

Deleted: Both commercial products, purchased by NASA, are found to have an improved lower atmospheric penetration capability over the Arctic Ocean compared to contemporaneous MetOp observations from EUMETSAT

Deleted: as evidenced by lower minimum penetration depths achieved over the frozen Arctic Ocean and higher penetration probability at the standard cut-of altitude of 500 m.

Deleted: , as compared to 60% MetOp observations that can measure PBL properties as low as 500 m

Deleted: resulting

Deleted: , however, seems relatively independent of this advancement

Deleted: Overall, the monthly mean PBLH pattern and seasonal evolution over the Arctic Ocean are best represented by NASA GeoOptics

Formatted: Indent: First line: 0.5"

Deleted: and MetOp data, in agreement with MERRA-2

Deleted: On the other hand

Deleted: ,

Deleted: retrieved from NASA Spire data

Deleted: , despite having improved lower tropospheric penetration, has insufficient spatial granularity and seasonality which is better represented in other datasets.

Deleted: In fact, the rate of decline of RO penetration within the PBL appears to be an influential factor affecting the choice of the minimum required RO penetration altitude (cut-off altitude) for PBLH retrieval. For products in which the rate of decline is smooth, the standard cut-off altitude for RO penetration depth (i.e. 500 m) works well, however, for products such as NASA Spire, where the rate of decline is drastic within the lowest 500 meters, the PBLH representation is improved when a lower cut-off altitude (i.e. 300 m) is used. Regardless, the spatiotemporal variability and qualitative representation of the Arctic PBLH appears to be independent of the choice of cut-off altitude threshold. A preliminary comparison with NOAA Spire data suggests that the refractivity-based PBLH is more sensitive to the choice of processing software used for retrieving bending angle profiles. The methodology used to obtain neutral atmosphere products from excess phase data is thus crucial for both lower tropospheric penetration probability and for Arctic PBLH representation. ...

Deleted: ,

Basha, G. and M.V. Ratnam (2009). Identification of atmospheric boundary layer height over a tropical station using high-resolution radiosonde refractivity profiles: Comparison with GPS radio occultation measurements, Journal of Geophysical Research, 114, https://doi.org/10.1029/2008jd011692.

Bowler, N. E. (2020). An assessment of GNSS radio occultation data produced by Spire, *Quarterly Journal of the Royal Meteorological Society, 146 (733),* 3772–3788.

Chang, H., J. Lee, H. Yoon, Y. J. Morton, and A. Saltman (2022). Performance assessment of radio occultation data from GeoOptics by comparing with COSMIC data. *Earth, Planets and Space, 74,* 108.

Ding, F., L. Iredell, M. Theobald, J. Wei, and D. Meyer (2021). PBL Height From AIRS, GPS RO, and MERRA-2 Products in NASA GES DISC and Their 10-Year Seasonal Mean Intercomparison, *Earth and Space Science, 8,* e2021EA001859, https://doi.org/10.1029/2021EA001859.

Ganeshan, M., & D. L. Wu (2015). An investigation of the Arctic inversion using COSMIC RO observations. *Journal of Geophysical Research: Atmospheres*, *120*(18), 9338-9351.

Ganeshan, M., & Y. Yang (2019). Evaluation of the Antarctic boundary layer thermodynamic structure in MERRA2 using dropsonde observations from the Concordiasi campaign. *Earth and Space Science*, *6*(12), 2397-2409.

Gelaro, R., McCarty, W., Suárez, M. J., Todling, R., Molod, A., Takacs, L., ... & Zhao, B. (2017). The modern-era retrospective analysis for research and applications, version 2 (MERRA-2). *Journal of climate*, *30*(14), 5419-5454.

Guo, P., Y.-H. Kuo, S. V. Sokolovskiy, and D. H. Lenschow (2011). Estimating atmospheric boundary layer depth using COSMIC radio occultationdata,J. Atmos. Sci.,68,1703–1713, doi:10.1175/2011JAS3612.1.

Innerkofler, J., G. Kirchengast, M. Schwärz, C. Marquardt, and Y. Andres (2023). GNSS radio occultation excess-phase processing for climate applications including uncertainty estimation, *Atmos. Meas. Tech., 16,* 5217–5247, https://doi.org/10.5194/amt-16-5217-2023, 2023.

Jensen, A. S., Lohmann, M. S., Nielsen, A. S., and Benzon, H.-H. (2004). Geometrical optics phase matching of radio occultation signals, Radio Science, 39, n/a-n/a, https://doi.org/10.1029/2003rs002899.

Deleted: ,

Formatted: Font: Not Italic, Complex Script Font: Not Italic

Formatted: Font: Not Italic, Complex Script Font: Not Italic

Deleted: ,

Deleted: :

Deleted: .

Deleted: ¶

Formatted: Font: Italic, Complex Script Font: Italic

Deleted: ,

Formatted: Font: Italic, Complex Script Font: Italic

Deleted: ¶
E. Bowler, N. (2020). An assessment of GNSS radio occultation data produced by Spire. *Quarterly Journal of the Royal Meteorological Society*, *146*(733), 3772-3788.¶

Deleted: , D. L.

Formatted: German

Deleted: , Y.

Formatted: Norwegian Bokmål

Deleted: ,

Formatted: Font: Italic, Complex Script Font: Italic

Deleted: ¶
Jarraud, M.: Guide to meteorological instruments and methods of observation (WMO-No. 8). *World Meteorological Organisation: Geneva, Switzerland*, *29*.¶

Kalmus, P., Ao, C. O., Wang, K.-N., Manzi, M. P., and Teixeira, J. (2022). A high-resolution planetary boundary layer height seasonal climatology from GNSS radio occultations, Remote Sensing of Environment, 276, 113037, https://doi.org/10.1016/j.rse.2022.113037.

Lock, A. P., Brown, A. R., Bush, M. R., Martin, G. M., & Smith, R. N. B. (2000). A new boundary layer mixing scheme. Part I: Scheme description and single-column model tests. *Monthly Weather Review*, **138**, 3187–3199.

Louis, J. F. (1982). A short history of the operational PBL parameterization at ECMWF. In *Workshop on Planetary Boundary Layer Parameterization, ECMWF, England, 1982*.

Deleted: ¶
Maturilli, M., Holdridge, D. J., Dahlke, S., Graeser, J., Sommerfeld, A., Jaiser, R., Deckelmann, H., Schulz, A.: Initial radiosonde data from 2019-10 to 2020-09 during project MOSAiC. *Alfred Wegener Institute, Helmholtz Centre for Polar and Marine Research, Bremerhaven*, *PANGAEA*, https://doi.org/10.1594/PANGAEA.928656, 2021¶
¶
Männel, B., Zus, F., Dick, G., Glaser, S., Semmling, M., Balidakis, K., ... & Schuh, H.: GNSS-based water vapor estimation and validation during the MOSAiC expedition. *Atmospheric Measurement Techniques*, *14*(7), 5127-5138, 2021.¶

McGrath-Spangler, E. L., Molod, A., Ott, L. E., & Pawson, S. (2015). Impact of planetary boundary layer turbulence on model climate and tracer transport. *Atmospheric Chemistry and Physics*, *15*(13), 7269-7286.

National Academies of Sciences, Engineering, and Medicine. (2018). *Thriving on our changing planet: A decadal strategy for earth observation from Space*. The National Academies Press. https://doi.org/10.17226/24938

Nelson, K. J., Xie, F., Ao, C. O., and Oyola-Merced, M. I. (2021). Diurnal Variation of the Planetary Boundary Layer Height Observed from GNSS Radio Occultation and Radiosonde Soundings over the Southern Great Plains, Journal of Atmospheric and Oceanic Technology, 38, 2081–2093, https://doi.org/10.1175/jtech-d-20-0196.1.

Qiu, C., Wang, X., Li, H., Zhou, K., Zhang, J., Li, Z., Liu, D., and Yuan, H. (2023). A Comparison of Atmospheric Boundary Layer Height Determination Methods Using GNSS Radio Occultation Data, *Atmosphere, 14*, 1654, https://doi.org/10.3390/atmos14111654.

Formatted: Font: Italic, Complex Script Font: Italic

ROM SAF (2019): ROM SAF Radio Occultation Interim Climate Data Record - Metop, EUMETSAT SAF on Radio Occultation Meteorology, DOI: 10.15770/EUM_SAF_GRM_0006. http://doi.org/10.15770/EUM_SAF_GRM_0006

Seidel, D. J., Ao, C. O., and Li, K. (2010). Estimating climatological planetary boundary layer heights from radiosonde observations: Comparison of methods and uncertainty analysis, *Journal of Geophysical Research, 115,* https://doi.org/10.1029/2009jd013680.

Formatted: Font: Italic, Complex Script Font: Italic

Seidel, D. J., Zhang, Y., Beljaars, A., Golaz, J.-C., Jacobson, A. R., and Medeiros, B. (2012). Climatology of the planetary boundary layer over the continental United States and Europe, *Journal of Geophysical Research: Atmospheres, 117,* https://doi.org/10.1029/2012jd018143.

Formatted: Font: Italic, Complex Script Font: Italic

Deleted: n/a-n/a,

Teixeira, J., Piepmeier, J., Nehrir, A., Ao, C., Chen, S., Clayson, C. A., et al. (2021). NASA planetary boundary layer (PBL) incubation study.

UCAR, "FORMOSAT-3/COSMIC-1 2021 Reprocessing Data Release", Nov 29 2022, FORMOSAT-3/COSMIC-1 2021 Reprocessing Data, https://data.cosmic.ucar.edu/gnss-ro/cosmic1/repro2021/UCAR_COSMIC1_2021_Repro_Notes.pdf. Access Date: 04/29/2024.

Winning, T. E., Chen, Y.-L., and Xie, F., (2017). Estimation of the marine boundary layer height over the central North Pacific using GPS radio occultation, *Atmospheric Research, 183,* 362–370, https://doi.org/10.1016/j.atmosres.2016.08.005

Wu, D. L., Gong, J., & Ganeshan, M. (2022). GNSS-RO Deep Refraction Signals from Moist Marine Atmospheric Boundary Layer (MABL). *Atmosphere*, *13*(6), 953.

Field Code Changed

Formatted: Font: Italic, Complex Script Font: Italic

Page 16: [1] Deleted	**Ganeshan, Manisha (GSFC-613.0)[MORGAN STATE UNIV.]**	**1/22/25 7:37:00 AM**

Page 16: [2] Deleted	**Ganeshan, Manisha (GSFC-613.0)[MORGAN STATE UNIV.]**	**1/21/25 5:39:00 PM**

Page 16: [3] Deleted	**Ganeshan, Manisha (GSFC-613.0)[MORGAN STATE UNIV.]**	**1/21/25 5:40:00 PM**

Page 16: [4] Deleted	**Ganeshan, Manisha (GSFC-613.0)[MORGAN STATE UNIV.]**	**1/24/25 1:09:00 AM**

Page 16: [5] Deleted	**Ganeshan, Manisha (GSFC-613.0)[MORGAN STATE UNIV.]**	**1/22/25 7:49:00 AM**

Page 16: [6] Deleted	**Ganeshan, Manisha (GSFC-613.0)[MORGAN STATE UNIV.]**	**1/22/25 8:18:00 AM**

Page 16: [7] Deleted	**Ganeshan, Manisha (GSFC-613.0)[MORGAN STATE UNIV.]**	**1/21/25 8:18:00 PM**